CELL CYCLE
2021, VOL. 20, NO. 13, 1334–1346
https://doi.org/10.1080/15384101.2021.1941612

Taylor & Francis
Taylor & Francis Group

RESEARCH PAPER

Circ_0006988 promotes the proliferation, metastasis and angiogenesis of non-small cell lung cancer cells by modulating miR-491-5p/MAP3K3 axis

Chao Yang, Jiang Shi, Jie Wang, Dexun Hao, Jinlu An, and Junguang Jiang

Department of Geriatric Respiratory Medicine, The First Affiliated Hospital of Zhengzhou University, Zhengzhou, China

ABSTRACT

Circular RNAs (circRNAs) are related to the progression of non-small cell lung cancer (NSCLC). However, the roles and mechanism of circ_0006988 are largely unknown. The levels of circ_0006988, Low-Density Lipoprotein Receptor Class A Domain Containing 3 (LDLRAD3), microRNA-491-5p (miR-491-5p), Mitogen-Activated Protein Kinase Kinase Kinase 3 (MAP3K3) were measured using quantitative real-time polymerase-chain reaction (qRT-PCR) and western blot assay. The characteristic of circ_0006988 was analyzed by RNase R assay and Actinomycin D assay. Functional analyses were processed by Cell Counting Kit-8 (CCK-8) assay, 5-ethynyl-2′-deoxyuridine (EdU) assay, colony formation assay, flow cytometry analysis, transwell assay, wound-healing assay and tube formation assay. The interactions between circ_0006988 and miR-491-5p as well as miR-491-5p and MAP3K3 were analyzed by dual-luciferase reporter assay and RNA immunoprecipitation (RIP) assay. Murine xenograft model assay was processed to verify the function of circ_0006988 *in vivo*. Immunohistochemistry (IHC) assay was conducted to examine the level of Ki67. Circ_0006988 abundance was increased in NSCLC tissues and cells. Circ_0006988 silencing restrained NSCLC cell proliferation, migration, invasion and angiogenesis, and induced apoptosis. Circ_0006988 sponged miR-491-5p, which directly targeted MAP3K3. MiR-491-5p overexpression repressed NSCLC cell malignant behaviors. MiR-491-5p downregulation or MAP3K3 overexpression reversed the effect of circ_0006988 silencing on NSCLC cell progression. In addition, circ_0006988 knockdown reduced xenograft tumor growth. ssCirc_0006988 contributed to the development of NSCLC by miR-491-5p/MAP3K3 axis.

ARTICLE HISTORY
Received 14 April 2021
Revised 31 May 2021
Accepted 8 June 2021

KEYWORDS
NSCLC; circ_0006988; miR-491-5p; MAP3K3

Introduction

Non-small cell lung cancer (NSCLC) is a usual type of lung cancer, posing a great threat to people's health and life [1,2]. Although huge improvements have gained on the therapy of NSCLC, the metastasis and recurrence make NSCLC therapy particularly difficult [3,4]. At present, molecular targeted therapy has become one of the important methods for advanced NSCLC therapy [5]. Hence, exploring the mechanism of NSCLC progression and identifying novel targets for improving the cure rate of this disease are crucial.

Circular RNAs (circRNAs, covalently closed non-coding RNA molecules) have been gradually identified to be involved in the regulation of diverse cellular functions and participate in human cancer progression [6,7]. More importantly, circRNAs can alter gene expression by interacting with microRNAs (miRNAs) via competitive endogenous RNAs (ceRNAs) mechanism [8]. Currently, the participation of circRNAs in NSCLC has been reported. For example, circ_0008003 exhibited an oncogenic role in NSCLC via miR-488/ZNF281 pathway [9]. Circ_0016760 aggravated the malignancy of NSCLC by decoying miR-4295 and elevating E2F3 [10]. As a member of circRNAs, circ_0006988, also termed as circ-Low Density Lipoprotein Receptor Class A Domain Containing 3 (circ-LDLRAD3), has been reported to serve as an accelerator in gastric cancer [11], pancreatic cancer [12] as well as NSCLC [13]. Even so, how circ_0006988 takes part in the development of NSCLC is largely unclear.

MiRNAs are short non-coding RNA molecules that act as vital players in tumorigenesis [14]. MiR-491-5p is an important biomarker and

CONTACT Junguang Jiang yc16603870103@163.com Department of Geriatric Respiratory Medicine The First Affiliated Hospital of Zhengzhou University, Zhengzhou, Henan, China
Supplemental data for this article can be accessed here

a tumor repressor in cancers, such as oral squamous cell carcinoma [15], osteosarcoma [16], gastric cancer [17] and bladder cancer [18]. Furthermore, miR-491-5p could hamper the growth and invasion of NSCLC by reducing IGF2BP1 [19]. However, the association of circ_0006988 and miR-491-5p in NSCLC development is unacknowledged.

Mitogen-Activated Protein Kinase Kinase Kinase 3 (MAP3K3) possesses a vital role in the development of cancers [20,21]. Moreover, MAP3K3 was linked to tumor cell growth, apoptosis and motility in NSCLC [22,23]. By using online tool starbase, miR-491-5p was discovered to share the binding sites of circ_006988 and MAP3K3, but their relationships in NSCLC development are uncertain.

In the present research, we focused on the impact of circ_0006988 on NSCLC development and the relationship of circ_0006988, miR-491-5p and MAP3K3 in NSCLC.

Materials and methods

Tissue samples acquisition

Tumor tissues and adjacent normal tissues were acquired from NSCLC patients (n = 40) at the First Affiliated Hospital of Zhengzhou University and frozen at −80°C. Written informed consents were offered by the participants. The research obtained approval from the Ethics Committee of the First Affiliated Hospital of Zhengzhou University.

Cell culture

Human bronchial epithelial cells (BEAS-2B) and NSCLC cells (A549 and H1299) were obtained from Procell (Wuhan, China). NSCLC cell line H1521 was bought from COBIOER (Nanjing, China). The RPMI 1640 medium (procell) plus 10% fetal bovine serum (Procell) and 1% penicillin/streptomycin (Procell) was utilized to culture the cells at 37°C and 5% CO_2.

Quantitative real-time polymerase chain reaction (qRT-PCR)

After being isolated via TRIzol (Invitrogen, Carlsbad, CA, USA), the RNA was subjected to PrimeScript RT kit (Takara, Dalian, China) or PrimeScript miRNA RT-PCR kit (Takara) for cDNA generation. Thereafter, qRT-PCR reaction was implemented via SYBR Premix Ex Taq II (Takara) and related primers (RIBOBIO, Guangzhou, China). The $2^{-\Delta\Delta Ct}$ method was adopted to compute relative expression. The primers were: circ_0006988: (F: 5′-CTGCAACGTCACCTACAACG-3′ and R: 5′-CACCACCAGCACAAAAATGA-3′); LDLRAD3: (F: ′-CAATGAGTGCAACATACCAGGC-3′ and R: 5′-ACTCTTGTCGAAGCAGTCAGG-3′); miR-491-5p: (F: 5′-GGAGTGGGGAACCCTTCC-3′ and R: 5′-GTGCAGGGTCCGAGGT-3′); MAP3K3: (F: 5′-GGCGAATTATAGCGTTCAGCC-3′ and R: 5′-GGGACAACAGCAATATCCTAAGG-3′); GAPDH: (F: 5′-CTCCTCCACCTTTGACGCT-3′ and R: 5′-GGGTCTCTCTCTTCCTCTTGTG-3′); U6: (F: 5′-CCTCGCTTCGGCAGCACATA-3′ and R: 5′-ACGCTTCACGAATTTGCGT-3′). GAPDH or U6 served as the internal control.

RNase R assay and Actinomycin D (Act D) assay

RNase R experiment was conducted by treating the RNA with RNase R (Epicenter, Madison, WI, USA) for 15 min. Act assay was implemented through exposing A549 and H1299 cells into Act D (Sigma-Aldrich, St. Louis, MO, USA) for indicated times. Thereafter, the expression of circ_0006988 and LDLRAD3 was examined with the aforementioned qRT-PCR.

Cell transfection

Circ_0006988 small interference RNA (si-circ_0006988), circ_0006988 short hairpin RNA (sh-circ_0006988) and sh-NC, circ_0006988 overexpression vector (circ_0006988) and related controls (si-NC and pCD-ciR), miR-491-5p inhibitor and inhibitor NC, miR-491-5p mimic and mimic

NC, MAP3K3 overexpression vector (MAP3K3) and its control (vector) were designed by RIBOBIO. Then cell transfection experiment was manipulated by Lipofectamine 2000 (Invitrogen).

Cell proliferation measurement

The cell proliferation capacity was tested by Cell Counting Kit-8 (CCK-8) assay, 5-ethynyl-2′- deoxyuridine (EdU) assay and Colony formation assay.

To conduct CCK-8 assay, NSCLC cells with various transfection were plated into 96-well plates and cultured with CCK-8 (Sigma-Aldrich) for 4 h at indicated time points. Then the absorption was examined at 450 nm utilizing a microplate reader (Bio-Rad, Hercules, CA, USA).

To conduct EdU assay, the EdU assay kit purchased from RIBOBIO was utilized. The transfected cells grown in 24-well plates were nurtured with EdU for 2 h, fixed with 4% paraformaldehyde (Sigma-Aldrich) for 15 min and then interacted with 0.5% Triton-X-100 for 15 min. After that, the cells were dyed with Apollo and DAPI. After the images were acquired under a Fluorescence microscope (Olympus, Tokyo, Japan), EdU-positive cells were quantified.

Flow cytometry analysis

Annexin V-FITC/PI Apoptosis Kit (Beyotime, Shanghai, China) was employed to assess the apoptosis of A549 and H1299 cells strictly based on the protocols of manufacturers. The flow cytometry (BD Biosciences, Franklin Lakes, NJ, USA) was employed for cell apoptosis detection.

Western blot assay

The protein was extracted with RIPA (Sigma-Aldrich), subjected to SDS-PAGE (Beyotime) for separation and then transferred onto polyvinylidene difluoride membranes (Beyotime). Afterward, the membranes were blocked in 5% nonfat milk, maintained with primary antibodies against MAP3K3 (bs-18,781 R; Bioss, Beijing, China), proliferating cell nuclear antigen (PCNA; bs-2007 R; Bioss), BCL2-Associated X (Bax; bs-0127 R; Bioss), B-cell lymphoma-2 (Bcl-2; bs-4563 R; Bioss), and GAPDH (bs-2188 R; Bioss) and mouse anti-rabbit secondary antibody (bs-0295 M-HRP; Bioss). The blots were captured using the ECL system (Beyotime).

Measurement of caspase-3 activity

The acitivity of caspase-3 in A549 and H1299 cells was analyzed through the usage of caspase-3 Activity Assay Kit (ab252897; Abcam, Cambridge, MA, USA) according to the manufacturer's instructions.

Transwell assay

The transwell inserts (BD Biosciences) or Matrigel-covered inserts were used for the measurement of cell migration and invasion. In brief, the transfected cells in serum-free medium were added in the top chambers. The below chambers were filled with the complete culture medium. 24 h later, the cells migrated or invaded into the lower chambers were dyed with crystal violet (Solarbio, Beijing, China) and counted under a microscope (100×; Olympus).

Wound-healing assay

The cell migration capacity was evaluated by wound-healing experiment. Briefly, the transfected cells were incubated in 24-well plates until 90% confluence. A new pipette tip was utilized to create a scratch. The wound closure was recorded at 0 h or 24 h post-scratch.

Tube formation assay

Briefly, Matrigel-coated 96-well plates were polymerized for 30 min. HUVECs (Procell) were seeded into the well. Next, the transfected A549 and H1299 cells resuspended in culture medium were added into the plates. After 6 h, the number of tubes was examined with a fluorescence microscope (Olympus).

Subcellular fraction analysis

By using the PARIS Kit (Ambion, Austin, TX, USA), the cytoplasmic and nuclear RNAs were separated in line with the protocols. Thereafter,

qRT-PCR was done to examine the subcellular distribution of circ_0006988 in the nucleus and cytoplasm with GAPDH or U6 as the controls of cytoplasm and nucleus.

Dual-luciferase reporter assay

The luciferase reporter vectors circ_0006988 ^{WT} and MAP3K3 3′UTR^{WT} were constructed by introducing the fragments of circ_0006988 or MAP3K3 3′UTR (harboring miR-491-5p binding sites) into pmirGLO plasmid (Promega, Madison, WI, USA), while circ_0006988^{MUT} and MAP3K3 3′UTR^{MUT} were generated through mutating miR-491-5p binding sites. After A549 and H1299 cells were co-transfected with the plasmids and mimic NC/miR-491-5p mimic, Dual-Luciferase Reporter Assay Kit (Promega) was utilized for measuring luciferase intensity.

RNA immunoprecipitation (RIP) assay

The EZ-Magna RIP kit (Millipore, Billerica, MA, USA) was adopted for RIP test. In short, NSCLC cells lysed in RIP buffer were maintained with magnetic beads conjugated with anti-Ago2 (bs-20,459 R; Bioss) or anti-IgG (bs-0297P; Bioss). Afterward, the RNA was isolated from the beads and then circ_0006988, miR-491-5p and MAP3K3 levels were examined.

Murine xenograft model

We purchased the male BALB/c nude mice (n = 10) from Beijing Vital River Laboratory Animal Technology Co., Ltd. (Beijing, China) and assigned them into 2 groups. Next, the mice were treated with sh-NC or sh-circ_0006988 transfected A549 cells. After treatment for 7 days, tumor size (1/2 (length × width^2)) was computed every 7 days. The mice were killed after 28 days and tumors were weighed and preserved at −80°C for further usage. The animal study was approved by the Ethics Committee of Animal Research of the First Affiliated Hospital of Zhengzhou University.

Immunohistochemistry (IHC) assay

According to the previous study, the expression of Ki67 and MAP3K3 in the tumors from the mice was examined through IHC assay [24]. The used antibodies including Ki67 (bs-2130 R; Bioss), MAP3K3 (bs-18,781 R) and mouse anti-rabbit secondary antibody (bs-0295 M-HRP; Bioss).

Statistical analysis

Statistical analysis was executed using GraphPad Prism 7 (GraphPad Inc., La Jolla, CA, USA). All values obtained from 3 duplicates were presented as mean ± standard deviation. The comparison of means was done via Student's *t*-test or one-way analysis of variance. Spearman's correlation coefficient analysis was conducted to analyze the linear correlations among the levels of circ_0006988, miR-491-5p and MAP3K3 in NSCLC tissues. $P < 0.05$ was thought to be significant.

Results

Circ_0006988 was overexpressed in NSCLC tissues and cells

At the beginning of the study, circ_0006988 expression in NSCLC tissues was detected by qRT-PCR assay. The results showed that circ_0006988 was upregulated in NSCLC tissues in comparison with normal tissues (Figure 1(a)). Compared to BEAS-2B cells, circ_0006988 was highly expressed in A549, H1581 and H1299 cells (Figure 1(b)). Then RNase R assay showed that circ_0006988 could be barely digested by RNase R, while LDLRAD3 was markedly digested by RNase R (Figure 1(c and d)). Act D assay indicated that the half-life of circ_0006988 was longer than LDLRAD3 (Figure 1(e and f)). The results indicated that circ_0006988 was stable and might be involved in NSCLC development.

Circ_0006988 overexpression facilitated NSCLC cell proliferation and inhibited apoptosis

Next, the exact roles of circ_0006988 in NSCLC development were explored. As exhibited in Figure 2(a and b), si-circ_0006988 transfection led to a reduction of circ_0006988 level and

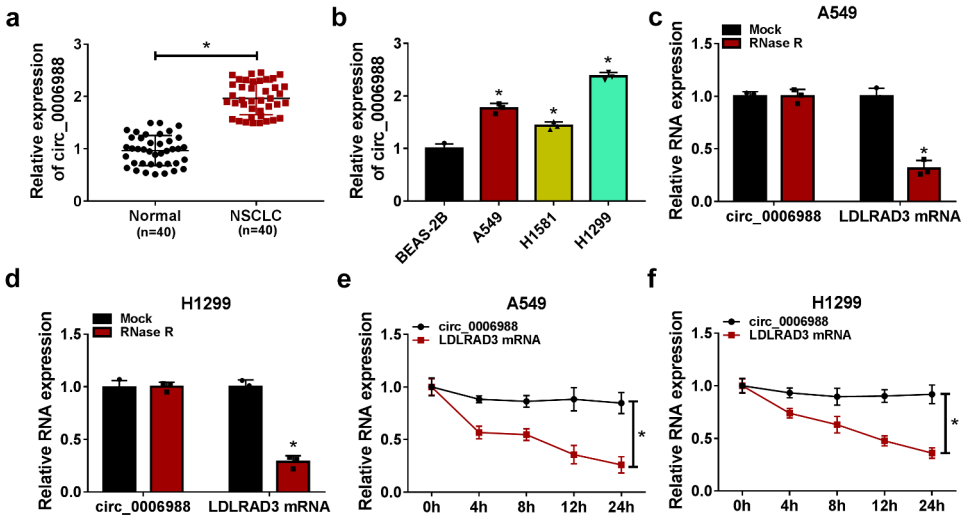

Figure 1. Circ_0006988 level was increased in NSCLC tissues and cells. (a) The expression of circ_0006988 in NSCLC tissues and normal tissues was detected by qRT-PCR assay. (b) The expression of circ_0006988 in BEAS-2B, A549, H1581 and H1299 cells was determined by qRT-PCR assay. (c and d) The levels of circ_0006988 and LDLRAD3 in A549 and H1299 cells treated with or without RNase R were detected by qRT-PCR assay. (e and f) The levels of circ_0006988 and LDLRAD3 in A549 and H1299 cells treated with Act D at indicated times were examined by qRT-PCR assay. *$P < 0.05$.

circ_0006988 overexpression vector transfection led to an elevation of circ_0006988 in both A549 and H1299 cells. Thereafter, the impacts of circ_0006988 knockdown and overexpression on NSCLC proliferation and apoptosis were investigated. As demonstrated by CCK-8 assay, circ_0006988 knockdown repressed cell viability and circ_0006988 overexpression promoted cell viability in both A549 and H1299 cells (Figure 2 (c and d)). EdU assay indicated that the proliferation of A549 and H1299 cells was suppressed by circ_0006988 silencing and was promoted by circ_0006988 elevation (Figure 2(e)). Colony formation assay showed that the colony formation ability of A549 and H1299 cells was repressed by decreasing circ_0006988 and was facilitated by increasing circ_0006988 (Figure 2(f)). Circ_0006988 deficiency induced cell apoptosis and circ_0006988 overexpression restrained cell apoptosis in A549 and H1299 cells, as illustrated by flow cytometry analysis (Figure 2(g)). Additionally, circ_0006988 interference reduced the protein levels of PCNA and Bcl-2 and increased the protein level of Bax in A549 and H1299 cells, while circ_0006988 overexpression showed that opposite results (Figure 2(h and i)). Furthermore, circ_0006988 knockdown increased caspase-3 activity, while circ_0006988 overexpression reduced caspase-3 activity in both A549 and H1299 cells (Figure S1A). All these findings suggested that circ_0006988 knockdown suppressed NSCLC cell growth and induced apoptosis.

Circ_0006988 overexpression promoted NSCLC migration, invasion and angiogenesis in NSCLC cells

The results of transwell assay showed that circ_0006988 silencing repressed the migration and invasion of A549 and H1299 cells, while circ_0006988 overexpression promoted the migration and invasion of A549 and H1299 cells (Figure 3(a and b)). Wound-healing assay presented that circ_0006988 knockdown inhibited A549 and H1299 cells to migrate, while circ_0006988 elevation exhibited the opposite results (Figure 3(c)). Furthermore, tube formation assay indicated that circ_0006988 silencing repressed the angiogenesis ability of HUVECs, whereas circ_0006988 overexpression promoted the angiogenesis ability of HUVECs (Figure 3 (d)). Collectively, circ_0006988 knockdown inhibited cell metastasis and angiogenesis in NSCLC cells.

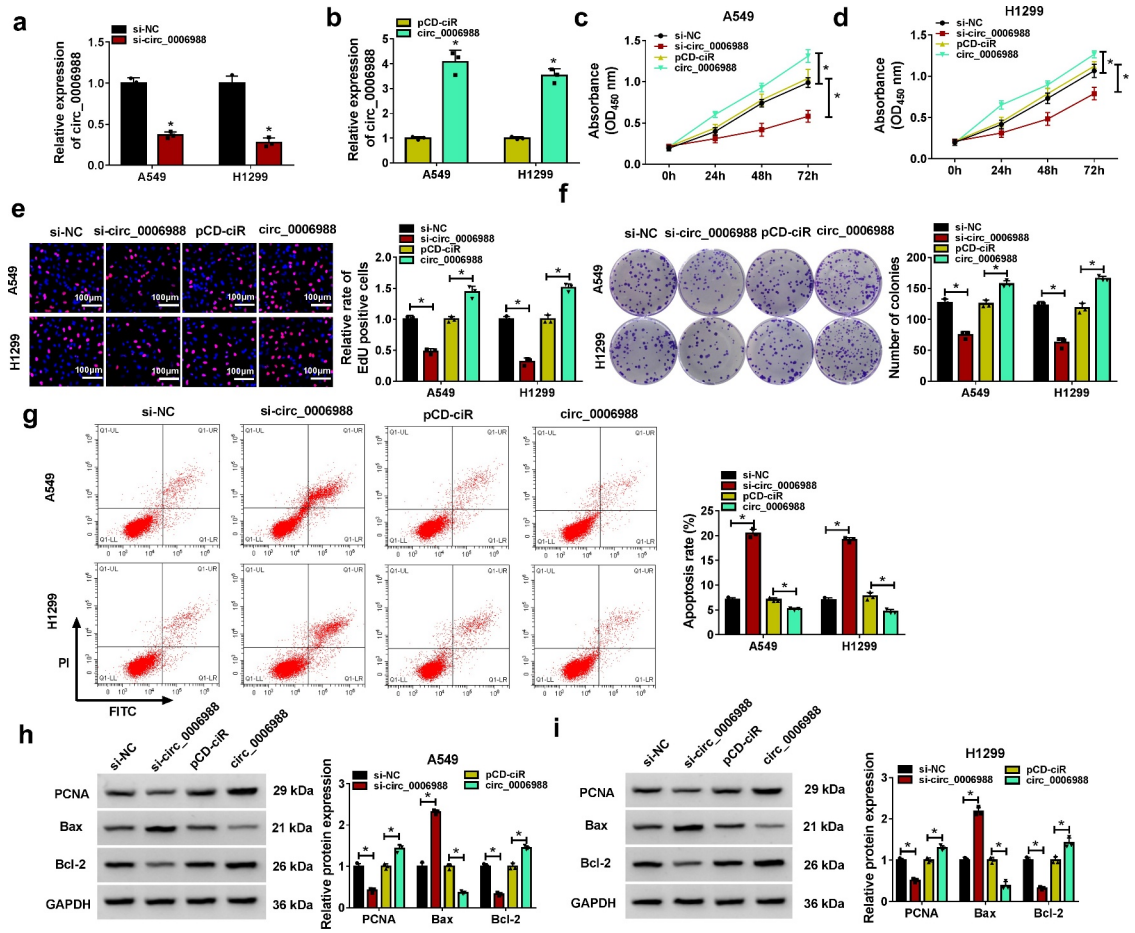

Figure 2. Effects of circ_0006988 overexpression or circ_0006988 knockdown on NSCLC cell proliferation and apoptosis. (a and b) The expression of circ_0006988 in A549 and H1299 cells transfected with si-NC, si-circ_0006988, pCD-ciR or circ_0006988 was detected by qRT-PCR assay. (c–i) A549 and H1299 cells were transfected with si-NC, si-circ_0006988, pCD-ciR or circ_0006988. (c–f) The proliferation ability of A549 and H1299 cells was assessed by CCK-8 assay, EdU assay and colony formation assay. (g) The apoptosis of A549 and H1299 cells was analyzed by flow cytometry analysis. (h and i) The protein levels of PCNA, Bax and Bcl-2 in A549 and H1299 cells were measured by western blot assay. *$P < 0.05$.

Circ_0006988 served as the sponge for miR-491-5p

Subcellular fraction analysis showed that circ_0006988 was mainly enriched in the cytoplasm of A549 and H1299 cells, indicating the potential of circ_0006988 served as miRNA sponges (Figure 4(a and b)). Through analyzing starbase(http://starbase.sysu.edu.cn/starbase2/), miR-491-5p was found to share the binding sites of circ_0006988 (Figure 4(c)). The transfection of miR-491-5p mimic markedly increased miR-491-5p expression in A549 and H1299 cells compared to mimic NC groups (Figure 4(d)). Then dual-luciferase activity assay exhibited that miR-491-5p overexpression repressed the luciferase activity of circ_0006988^{WT} but did not affect circ_0006988^{MUT} in A549 and H1299 cells (Figure 4(e and f)). RIP assay indicated that circ_0006988 and miR-491-5p were enriched in the immunoprecipitated complexes in anti-Ago2 groups compared to anti-IgG control groups (Figure 4(g and h)). These results demonstrated the interaction between circ_0006988 and miR-491-5p. Indeed, miR-491-5p was lowly expressed in NSCLC tissues and cells compared to normal tissues and cells (Figure 4(i and j)). Besides, our results showed that circ_0006988 knockdown increased miR-491-5p expression, while circ_0006988 overexpression reduced miR-491-5p expression in A549 and H1299 cells (Figure 4(k and l)). Collectively, circ_0006988 sponged miR-491-5p to alter miR-491-5p expression.

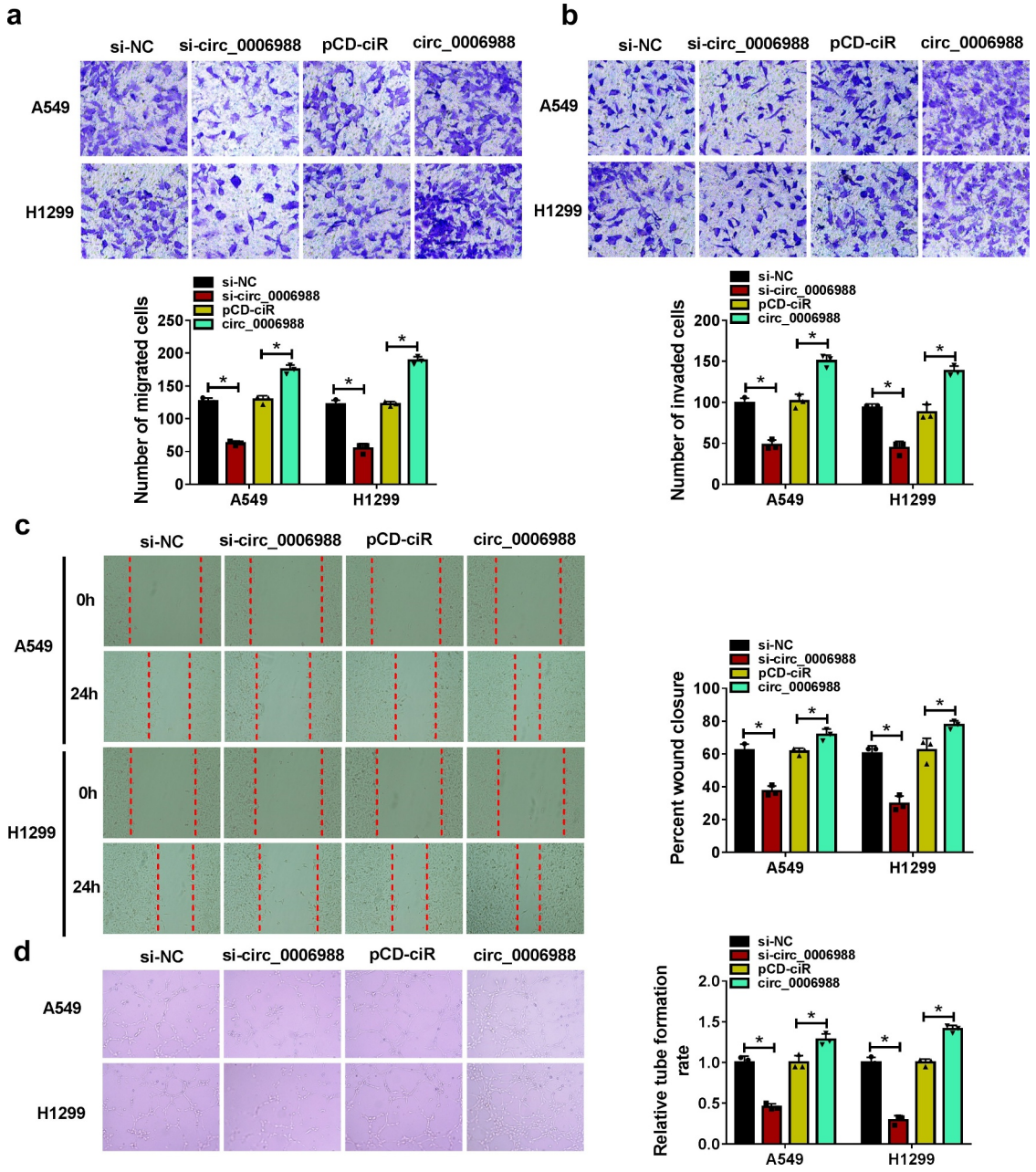

Figure 3. Impacts of circ_0006988 overexpression or knockdown on cell motility and angiogenesis in NSCLC cells. A549 and H1299 cells were transfected with si-NC, si-circ_0006988, pCD-ciR or circ_0006988. (a and b) The migration and invasion of A549 and H1299 cells were tested by transwell assay. (c) The migration ability of A549 and H1299 cells was assessed by wound-healing assay. (d) The tube formation ability of HUVECs was evaluated by tube formation assay. *$P < 0.05$.

Overexpression of miR-491-5p repressed cell proliferation, migration, invasion and angiogenesis and facilitated apoptosis in NSCLC cells

Subsequently, the functions of miR-491-5p in NSCLC cell progression were explored. As demonstrated by CCK-8 assay, EdU assay and colony formation assay, overexpression of miR-491-5p apparently suppressed the ability of A549 and H1299 cells to proliferate compared to mimic NC control groups (Figure 5(a–d)). Flow cytometry indicated that miR-491-5p elevation triggered the apoptosis of A549 and H1299 cells compared to control groups (Figure 5(e)). Moreover, our results showed that miR-491-5p overexpression reduced the protein levels of PCNA and Bcl-2 and elevated the protein level of Bax in both A549 and H1299 cells (Figure 5(f and g)). Overexpression of miR-491-5p also facilitated the activity of caspase-3 in A549 and

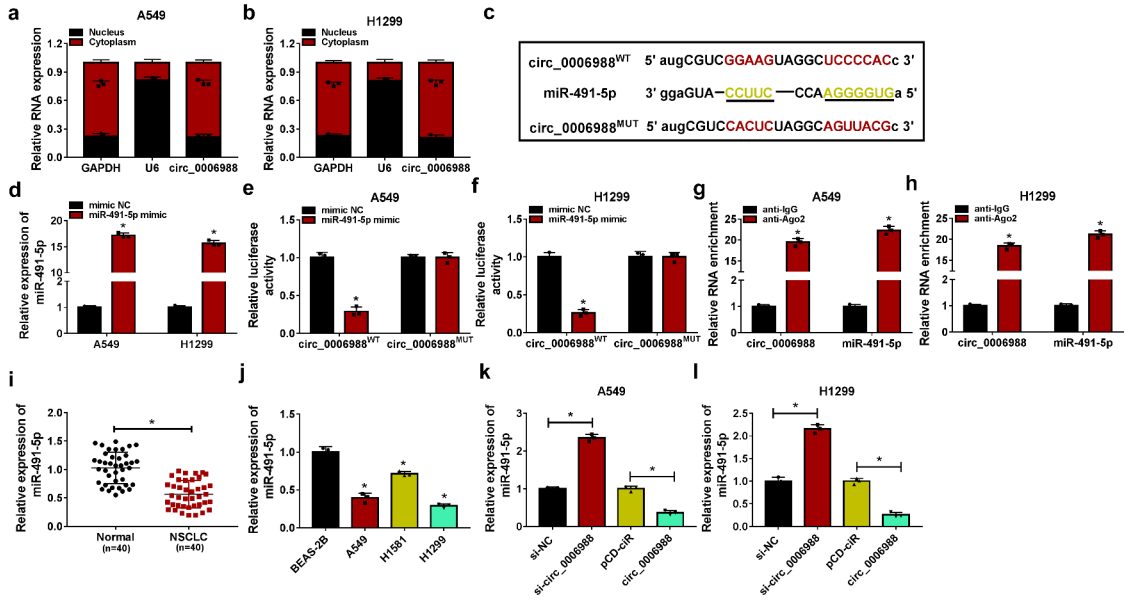

Figure 4. Circ_0006988 directly interacted with miR-491-5p. (a and b) The expression of circ_0006988 in the nucleus and cytoplasm of A549 and H1299 cells was analyzed by Subcellular fraction analysis. (c) MiR-491-5p contained the binding sites of circ_0006988. (d) The expression of miR-491-5p in A549 and H1299 cells transfected with mimic NC or miR-491-5p mimic was detected by qRT-PCR assay. (e–h) The combination between circ_0006988 and miR-491-5p was analyzed by dual-luciferase reporter assay and RIP assay. (i and j) The expression of miR-491-5p in NSCLC tissues and cells was determined by qRT-PCR assay. (k and l) After A549 and H1299 cells were transfected with si-NC, si-circ_0006988, pCD-ciR or circ_0006988, the expression of miR-491-5p was determined by qRT-PCR assay. *$P < 0.05$.

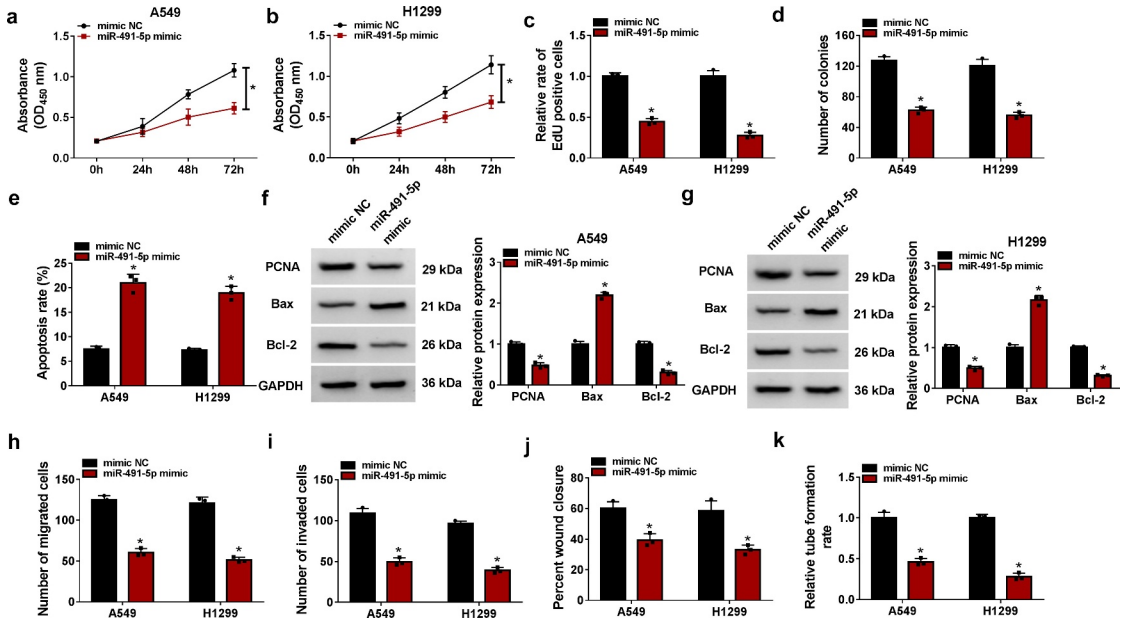

Figure 5. Effects of miR-491-5p on cell proliferation, apoptosis, metastasis and angiogenesis in NSCLC cells. A549 and H1299 cells were transfected with mimic NC or miR-491-5p. (a-d) The proliferation ability of A549 and H1299 cells was assessed by CCK-8 assay, EdU assay and colony formation assay. (e) The apoptosis of A549 and H1299 cells was analyzed by flow cytometry analysis. (f and g) The protein levels of PCNA, Bax and Bcl-2 in A549 and H1299 cells were measured by western blot assay. (h and i) The migration and invasion of A549 and H1299 cells were evaluated by transwell assay. (j) The migration capacity of A549 and H1299 cells was tested by wound-healing assay. (k) The angiogenesis of HUVECs was assessed by tube formation assay. *$P < 0.05$.

H1299 cells (Figure S1B). As demonstrated by transwell assay and wound-healing assay, miR-491-5p overexpression restrained the migration and invasion abilities of A549 and H1299 cells compared to mimic NC control groups (Figure 5(h–j)). Additionally, the tube formation ability of HUVECs was blocked by increasing miR-491-5p (Figure 5(k)). Taken together, miR-491-5p overexpression inhibited the malignant behaviors of NSCLC cells.

MAP3K3 was the target gene of miR-491-5p

By using starbase, we found that MAP3K3 was the target gene of miR-491-5p (Figure 6(a)). To verify the prediction, dual-luciferase reporter assay and RIP assay were performed. Dual-luciferase reporter assay showed that the luciferase activity of MAP3K3 3′UTR^{WT} in A549 and H1299 cells was inhibited after miR-491-5p overexpression, while the luciferase activity of MAP3K3 3′UTR^{MUT} was not affected (Figure 6(b and c)). RIP assay showed

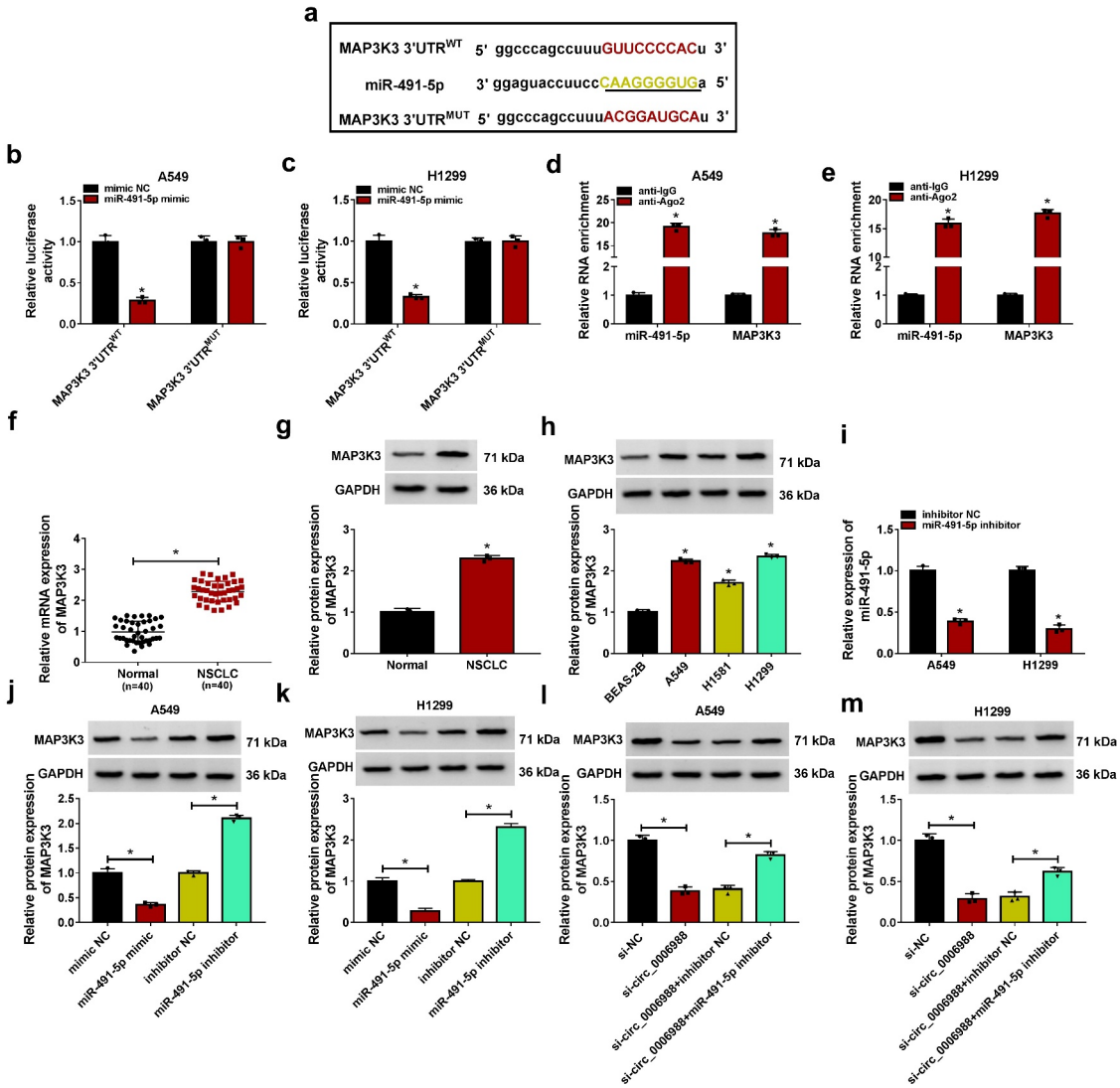

Figure 6. MiR-491-5p directly interacted with miR-491-5p. (a) The binding sites between miR-491-5p and MAP3K3. (b–e) Dual-luciferase reporter assay and RIP assay were manipulated for the relationship between miR-491-5p and MAP3K3. (f and g) The mRNA and protein levels of MAP3K3 in NSCLC tissues and normal tissues were measured by qRT-PCR assay and western blot assay, respectively. (h) The protein level of MAP3K3 in BEAS-2B, A549, H1581 and H1299 cells was measured via western blot assay. (i) The expression of miR-491-5p in A549 and H1299 cells transfected with inhibitor NC or miR-491-5p inhibitor was determined by qRT-PCR assay. (j and k) The protein level of MAP3K3 in A549 and H1299 cells transfected with mimic NC, miR-491-5p mimic, inhibitor NC or miR-491-5p inhibitor was measured by western blot assay. (l and m) After A549 and H1299 cells were transfected with si-NC, si-circ_0006988, si-circ_0006988+ inhibitor NC or si-circ_0006988+ miR-491-5p inhibitor, the protein level of MAP3K3 was examined via western blot assay. *$P < 0.05$.

that the enrichment of miR-491-5p and MAP3K3 was increased in anti-Ago2 RIP groups compared to anti-IgG RIP groups (Figure 6(d and e)). As expected, the mRNA and protein levels of MAP3K3 were elevated in NSCLC tissues in comparison with normal tissues (Figure 6(f and g)). Compared to BEAS-2B cells, MAP3K3 protein level was increased in A549, H1581 and H1299 cells (Figure 6(h)). As presented in Figure 6(i), miR-491-5p inhibitor transfection led to a reduction in miR-491-5p level in A549 and H1299 cells relative to inhibitor NC groups (Figure 6(i)). Moreover, it was found that miR-491-5p overexpression decreased MAP3K3 protein level and miR-491-5p inhibition increased MAP3K3 protein level in A549 and H1299 cells (Figure 6(j and k)). Of note, our results showed that circ_0006988 silencing reduced the protein level of MAP3K3 in A549 and H1299 cells, while miR-491-5p inhibition reversed the effect (Figure 6(l) and m). Besides, our results showed that miR-491-5p level was negatively correlated with circ_0006988 and MAP3K3 level, and circ_0006988 level was positively correlated with MAP3K3 level in NSCLC tissues (Figure S2A-C). To sum up, circ_0006988 directly targeted miR-491-5p to modulate MAP3K3 expression.

MiR-491-5p inhibition or MAP3K3 overexpression reversed the impacts of circ_0006988 silencing on NSCLC malignant behaviors

As presented in Figure 7(a), MAP3K3 overexpression vector transfection caused a significant elevation of MAP3K3 protein level in A549 and H1299 cells. Next, the relationship between circ_0006988 and miR-491-5p or MAP3K3 in regulating NSCLC progression was investigated. As illustrated by CCK-8 assay, EdU assay and colony formation assay, circ_0006988 apparently inhibited the proliferation of A549 and H1299 cells, while miR-491-5p inhibition or MAP3K3 overexpression weakened the effect (Figure 7(b–e)). Flow cytometry analysis indicated that the promotional effect of circ_0006988 deficiency on the apoptosis in A549 and H1299 cells was reversed by decreasing miR-491-5p or increasing MAP3K3 (Figure 7(f)). Western blot assay showed that miR-491-5p inhibition or MAP3K3 elevation ameliorated the effects of circ_0006988 silencing on PCNA, Bax and Bcl-2 protein levels in A549 and H1299 cells (Figure 7(g and h)). Moreover, the promotional effect of circ_0006988 knockdown on caspase-3 activity was weakened by miR-491-5p inhibition or MAP3K3 elevation (Figure S1C). The results of transwell assay and wound-healing assay indicated

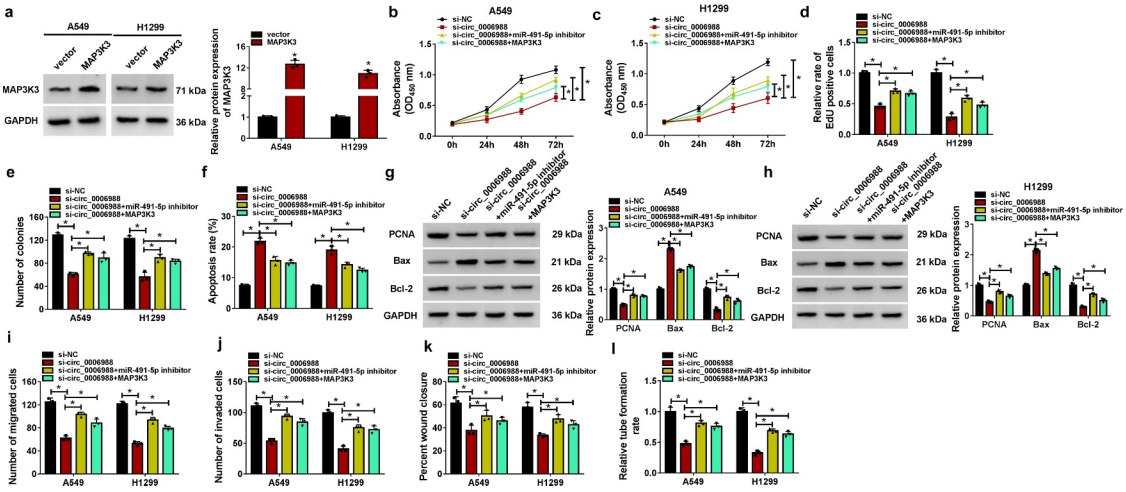

Figure 7. MiR-491-5p inhibition or MAP3K3 elevation reversed the effects of circ_0006988 on NSCLC cell growth, apoptosis, metastasis and angiogenesis. (a) The protein level of MAP3K3 in A549 and H1299 cells transfected with MAP3K3 or vector was measured via western blot assay. (b–l) A549 and H1299 cells were transfected with si-NC, si-circ_0006988, si-circ_0006988+ miR-491-5p inhibitor or si-circ_0006988+ MAP3K3. (b–e) The proliferation of A549 and H1299 cells was assessed by CCK-8 assay, EdU assay and colony formation assay. (f) The apoptosis of A549 and H1299 cells was analyzed by flow cytometry analysis. (g and h) The protein levels of PCNA, Bax and Bcl-2 in A549 and H1299 cells were measured via western blot assay. (i–k) The migration and invasion of A549 and H1299 cells were evaluated by transwell assay and wound-healing assay. (l) The angiogenesis ability of HUVECs was analyzed by tube formation assay. *$P < 0.05$.

that the inhibitory effects of circ_0006988 interference on A549 and H1299 cell migration and invasion were reversed by the inhibition of miR-491-5p and the elevation of MAP3K3 (Figure 7(i–k)). In addition, circ_0006988 knockdown repressed the angiogenesis of HUVECs, while miR-491-5p inhibition or MAP3K3 overexpression rescued the effect (Figure 7(l)). These results suggested that circ_0006988 regulated NSCLC cell progression by altering miR-491-5p or MAP3K3 expression.

Circ_0006988 knockdown blocked tumor growth *in vivo*

Finally, the function of circ_0006988 in tumorigenesis *in vivo* was explored. It was found that circ_0006988 knockdown inhibited tumor volume and weight compared to sh-NC control groups (Figure 8(a–c)). Moreover, the levels of circ_0006988, MAP3K3 mRNA and MAP3K3 protein were reduced and the level of miR-491-5p was elevated in the xenograft tumors of sh-circ_0006988 groups compared to sh-NC groups (Figure 8(d–g)). In addition, IHC assay showed that circ_0006988 knockdown inhibited the levels of Ki67 and MAP3K3 in the xenograft tumors of sh-circ_0006988 groups compared to sh-NC groups (Figure 8(h and i)). Western blot assay indicated that Bax protein level was increased and Bcl-2 protein level was decreased in the xenograft tumors by circ_0006988 knockdown (Figure 8(j)). Collectively, circ_0006988 silencing blocked tumor formation *in vivo*.

Discussion

As a kind of novel identified non-coding RNAs, circRNAs are considered to be vital players in the carcinogenesis of NSCLC [25]. Here, we focused on the functions of circ_0006988 in NSCLC development. It was demonstrated that circ_0006988 functioned as an oncogenic drive in NSCLC via circ_0006988/miR-491-5p/MAP3K3 pathway, which was discovered for the first time.

Presently, the relationship between circRNAs and human cancers is a hot topic [26]. Wang *et al.* unraveled that circ-LADLRAD3 was overexpressed in gastric cancer and aggravated tumor cell metastasis and growth and curbed apoptosis via miR-224-5p/NRP2 [11]. Yao *et al.* manifested that circ-LADLRAD3 indicated the poor outcomes of pancreatic cancer patients and triggered tumor cell malignancy via adsorbing miR-137-3p and elevating PTN [12]. Moreover, circ-LDLRAD3

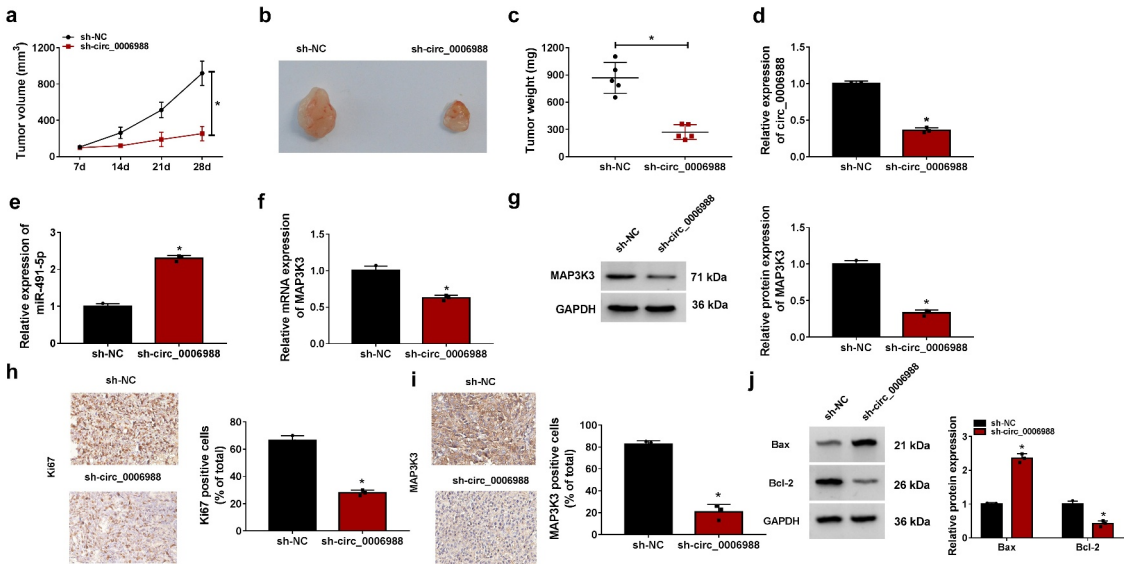

Figure 8. Circ_0006988 silencing inhibited tumor growth *in vivo*. (a–c) Tumor volume and weight were examined. (d–f) The levels of circ_0006988, miR-491-5p and MAP3K3 in the xenograft tumors were determined by qRT-PCR assay. (g) The protein level of MAP3K3 in the xenograft tumor was measured by western blot assay. (h and i) The levels of Ki67 and MAP3K3 in the xenograft tumors were estimated by IHC assay. (j) The protein levels of Bax and Bcl-2 in the xenograft tumors were detected by western blot assay. *$P < 0.05$.

abundance was increased in NSCLC and promoted the tumorigenesis through altering miR-137 and SLC1A5 [13]. In agreement with the previous, we also found that circ_0006988 was abnormally increased in NSCLC. Moreover, we verified that circ_0006988 interference led to evident suppression on NSCLC cell proliferation, invasion, migration and angiogenesis and marked acceleration on apoptosis *in vitro*. Of note, circ_0006988 enhancement exhibited the opposite results in NSCLC cell malignant phenotypes. Besides, we construct the xenograft model to better understand the role of circ_0006988 on NSCLC and found that circ_0006980 silencing blocked tumorigenesis of NSCLC *in vivo*. All these findings indicated the anti-tumor effect of circ_0006988 knockdown in NSCLC.

Subsequently, we validated that miR-491-5p could be sponged by circ_0006988. Multiple reports indicated the tumor-suppressive role of miR-491-5p [18,27–29]. Similarly, our research indicated that miR-491-5p addition restrained the growth, motility and angiogenesis and triggered the apoptosis of NSCLC cells, which was consistent with the former study [19]. Furthermore, miR-491-5p downregulation ameliorated the influence of circ_0006988 deficiency on NSCLC development, implying circ_0006988 alters NSCLC malignancy via adsorbing miR-491-5p.

Additionally, MAP3K3 was identified to be targeted by miR-491-5p. MAP3K3 has been documented to serve its oncogenic role via acting as the target of miRNAs, such as miR-212-3p [30], miR-4458 [31], miR-194 [32] and miR-188 [22]. However, the combination between miR-491-5p and MAP3K3 was found for the first time. We also found that circ_0006988 could regulate MAP3K3 expression with miR-491-5p as a crosstalk. Of note, our findings suggested that MAP3K3 overexpression weakened circ_0006988 silencing-mediated influence on NSCLC cell malignant behaviors. However, whether MAP3K3 alters miR-491-5p-mediated effects of NSCLC progression has been clarified.

Taken together, our study corroborated that circ_0006988 accelerated the deterioration of NSCLC by miR-491-5p/MAP3K3 axis, highlighting the potential of circ_0006988 to act as a therapeutic target for NSCLC.

Disclosure statement

No potential conflict of interest was reported by the author(s).

References

[1] Postmus PE, Kerr KM, Oudkerk M, et al. Early and locally advanced non-small-cell lung cancer (NSCLC): ESMO clinical practice guidelines for diagnosis, treatment and follow-up. Ann Oncol. 2017;28: iv1–iv21.

[2] Bray F, Ferlay J, Soerjomataram I, et al. Global cancer statistics 2018: GLOBOCAN estimates of incidence and mortality worldwide for 36 cancers in 185 countries. CA Cancer J Clin. 2018;68:394–424.

[3] Cheng H, Perez-Soler R. Leptomeningeal metastases in non-small-cell lung cancer. Lancet Oncol. 2018;19:e43–e55.

[4] Rusch VW. Stage III non-small cell lung cancer. Semin Respir Crit Care Med. 2016;37:727–735.

[5] Jonna S, Subramaniam DS. Molecular diagnostics and targeted therapies in non-small cell lung cancer (NSCLC): an update. Discov Med. 2019;27:167–170.

[6] Das A, Gorospe M, Panda AC. The coding potential of circRNAs. Aging (Albany NY). 2018;10:2228–2229.

[7] Patop IL, Kadener S. circRNAs in cancer. Curr Opin Genet Dev. 2018;48:121–127.

[8] Zhong Y, Du Y, Yang X, et al. Circular RNAs function as ceRNAs to regulate and control human cancer progression. Mol Cancer. 2018;17(1):79.

[9] Gu R, Shao K, Xu Q, et al. Circular RNA hsa_-circ_0008003 facilitates tumorigenesis and development of non-small cell lung carcinoma via modulating miR-488/ZNF281 axis. J Cell Mol Med. 2020. DOI:10.1111/jcmm.15987.

[10] Yan X, Wang T, Wang J. Circ_0016760 acts as a sponge of MicroRNA-4295 to enhance E2F transcription factor 3 expression and facilitates cell proliferation and glycolysis in nonsmall cell lung cancer. Cancer Biother Radiopharm. 2020. DOI:10.1089/cbr.2020.3621

[11] Wang Y, Yin H, Chen X. Circ-LDLRAD3 enhances cell growth, migration, and invasion and inhibits apoptosis by regulating MiR-224-5p/NRP2 axis in gastric cancer. Dig Dis Sci. 2021. DOI:10.1007/s10620-020-06733-1

[12] Yao J, Zhang C, Chen Y, et al. Downregulation of circular RNA circ-LDLRAD3 suppresses pancreatic cancer progression through miR-137-3p/PTN axis. Life Sci. 2019;239:116871.

[13] Xue M, Hong W, Jiang J, et al. Circular RNA circ-LDLRAD3 serves as an oncogene to promote non-small cell lung cancer progression by upregulating SLC1A5 through sponging miR-137. RNA Biol. 2020;17:1811–1822.

[14] Di Leva G, Garofalo M, Croce CM. MicroRNAs in cancer. Annu Rev Pathol. 2014;9:287–314.

[15] Huang WC, Chan SH, Jang TH, et al. miRNA-491-5p and GIT1 serve as modulators and biomarkers for oral squamous cell carcinoma invasion and metastasis. Cancer Res. 2014;74:751–764.
[16] Chen T, Li Y, Cao W, et al. miR-491-5p inhibits osteosarcoma cell proliferation by targeting PKM2. Oncol Lett. 2018;16:6472–6478.
[17] Zhang J, Ren J, Hao S, et al. MiRNA-491-5p inhibits cell proliferation, invasion and migration via targeting JMJD2B and serves as a potential biomarker in gastric cancer. Am J Transl Res. 2018;10:525–534.
[18] Liu F, Zhang H, Xie F, et al. Hsa_circ_0001361 promotes bladder cancer invasion and metastasis through miR-491-5p/MMP9 axis. Oncogene. 2020;39:1696–1709.
[19] Gong F, Ren P, Zhang Y, et al. MicroRNAs-491-5p suppresses cell proliferation and invasion by inhibiting IGF2BP1 in non-small cell lung cancer. Am J Transl Res. 2016;8:485–495.
[20] Zhang Y, Wang SS, Tao L, et al. Overexpression of MAP3K3 promotes tumour growth through activation of the NF-kappaB signalling pathway in ovarian carcinoma. Sci Rep. 2019;9:8401.
[21] Santoro R, Zanotto M, Carbone C, et al. MEKK3 sustains EMT and stemness in pancreatic cancer by regulating YAP and TAZ transcriptional activity. Anticancer Res. 2018;38:1937–1946.
[22] Zhao L, Ni X, Zhao L, et al. MiroRNA-188 acts as tumor suppressor in non-small-cell lung cancer by targeting MAP3K3. Mol Pharm. 2018;15:1682–1689.
[23] Tang H, Lv W, Sun W, et al. miR505 inhibits cell growth and EMT by targeting MAP3K3 through the AKTNFkappaB pathway in NSCLC cells. Int J Mol Med. 2019;43:1203–1216.
[24] Xing S, Qu Y, Li C, et al. Deregulation of lncRNA-AC078883.3 and microRNA-19a is involved in the development of chemoresistance to cisplatin via modulating signaling pathway of PTEN/AKT. J Cell Physiol. 2019;234:22657–22665.
[25] De Fraipont F, Gazzeri S, Cho WC, et al. Circular RNAs and RNA splice variants as biomarkers for prognosis and therapeutic response in the liquid biopsies of lung cancer patients. Front Genet. 2019;10:390.
[26] Zhang HD, Jiang LH, Sun DW, et al. CircRNA: a novel type of biomarker for cancer. Breast Cancer. 2018;25:1–7.
[27] Guo J, Luo C, Yang Y, et al. MiR-491-5p, as a tumor suppressor, prevents migration and invasion of breast cancer by Targeting ZNF-703 to regulate AKT/mTOR pathway. Cancer Manag Res. 2021;13:403–413.
[28] Wang Y, Wu Z, Li Y, et al. Long non-coding RNA H19 promotes proliferation, migration and invasion and inhibits apoptosis of breast cancer cells by targeting miR-491-5p/ZNF703 axis. Cancer Manag Res. 2020;12:9247–9258.
[29] Qi G, Li L. LncRNA TTN-AS1 promotes progression of non-small cell lung cancer via regulating miR-491-5p/ZNF503 axis. Onco Targets Ther. 2020;13:6361–6371.
[30] Zhang L, Zhang Y, Wang S, et al. MiR-212-3p suppresses high-grade serous ovarian cancer progression by directly targeting MAP3K3. Am J Transl Res. 2020;12:875–888.
[31] Gui D, Cao H. Long non-coding RNA CDKN2B-AS1 promotes osteosarcoma by increasing the expression of MAP3K3 via sponging miR-4458. In Vitro Cell Dev Biol Anim. 2020;56:24–33.
[32] Yin W, Shi L, Mao Y. MiR-194 regulates nasopharyngeal carcinoma progression by modulating MAP3K3 expression. FEBS Open Bio. 2019;9:43–52.